ENVIRONMENTAL FORENSICS
https://doi.org/10.1080/15275922.2026.2628337

Taylor & Francis
Taylor & Francis Group



# DN-PMF as a Sensitivity Test for Conventional PMF (C-PMF) Source Apportionment in Three Cities in South Africa, 2017–2018

Chantelle Howlett-Downing[a,b], Johan Boman[c], Peter Molnár[d], and Janine Wichmann[a]

[a]School of Health Systems and Public Health, Faculty of Health Sciences, University of Pretoria, Gezina, Pretoria, South Africa; [b]South African Medical Research Council, Environmental Health Unit, Climate Change and Health, Pretoria, South Africa; [c]Department of Chemistry and Molecular Biology, Atmospheric Science Division, University of Gothenburg, Göteborg, Sweden; [d]Department of Occupational and Environmental Medicine, Institute of Medicine, Sahlgrenska Academy, University of Gothenburg, Göteborg, Sweden

**ABSTRACT**

Source apportionment through factorization is a common method for identifying sources of air pollution. Both PCA and DN-PMF have assumptions, strengths, and limitations. Assigning sources to factors is inherently subjective and can introduce bias. PCA for the number of sources, C-PMF and DN-PMF is performed on data from three cities which were sampled at the same time, 16 April 2017 to 18 April 2018. The DN-PMF was able to give seasonal information to support the source apportionment. Results of the PCA included 6 factors for Thohoyandou and Pretoria and 7 factors for Cape Town. At the two large city sites, the C-PMF presented a dominant coal emissions source (29% and 35.6%) yearly and a strong biomass source during winter (24% and 17%). The dominant yearly source shifted to vehicular emissions with the DN-PMF model in Pretoria and Cape Town (41% and 12%) and coal burning at Thohoyandou (33%). By considering the mixing layer and meteorological conditions the factors shifted while keeping the dominant Cl-Pb and Cu-Zn tracer combinations.

**HIGHLIGHTS**

DN-PMF is a valid sensitivity test for C-PMF by reducing subjective bias during the assigning of sources to factors.

**KEYWORDS**

C-PMF; DN-PMF; $PM_{2.5}$; sensitivity study; sources

## 1. Introduction

Air pollution, particularly the presence of fine particulate matter (PM), poses a significant threat to public and environmental health. "Aerosolized" PM found in air streams is a complex mixture of both chemical and biological components that vary considerably with time, location, and meteorological conditions (Huang et al. 2021; Hueglin et al. 2005; Liang et al. 2015). The constituents of ambient PM include biological organisms (e.g., bacteria, fungi, and viruses), organic compounds (e.g., polycyclic aromatic hydrocarbons [PAHs] and their nitro-derivatives [NPAHs]), nitrates, sulphates, trace metals (e.g., iron, copper, nickel, zinc, and vanadium), and carbon-based species such as black carbon (BC) and organic carbon (Kumar et al. 2018; Lee et al. 2016).

These chemical components not only serve as markers for emission sources but are also relevant due to their toxicological properties. Their composition and concentrations differ markedly across urban, peri-urban, and rural landscapes, depending on proximity to industrial activities, transportation corridors, population density, and biomass use (Junker and Liousse 2008). Suspended PM is further categorized by aerodynamic diameter. Coarse particles ($PM_{10}$) range from 2.5 to 10 µm, while fine particles ($PM_{2.5}$) are smaller than 2.5 µm and are of particular concern due to their ability to penetrate deep into the human respiratory tract (Ruuskanen et al. 2001).

A key assumption of traditional receptor-based source apportionment techniques is that, although source factors are distinct and uncorrelated, the pollutant mixture is effectively homogeneous at the receptor point. In reality, meteorological variability influences ambient concentrations through changes in dispersion, transport, and

CONTACT Chantelle Howlett-Downing Chantelle.Howlett-Downing@mrc.ac.za South African Medical Research Council, 1 Soutpansberg Road, Pretoria 0001, South Africa

Supplemental data for this article can be accessed online at https://doi.org/10.1080/15275922.2026.2628337.

atmospheric mixing, in addition to emission rate changes. As a result, conventional positive matrix factorization (C-PMF) may lose information from the input data when concentration variability is dominated by meteorology-driven dilution rather than changes in emissions.

Dispersion-normalized positive matrix factorization (DN-PMF) was developed to address this limitation by incorporating a ventilation coefficient, thereby reducing first-order dilution effects prior to factorization. DN-PMF does not replace conventional PMF or introduce new source information; rather, it is applied as a diagnostic or sensitivity framework to evaluate how meteorology-driven dilution influences the stability and interpretability of PMF source attribution. Table 1 in this study, DN-PMF is applied to three previously sampled and analyzed sites in South Africa.

Taken together, the literature and results from this study indicate that DN-PMF is most appropriately used as a sensitivity tool applied alongside conventional PMF. Its added value is most evident in multi-site or policy-relevant studies where dispersion conditions differ substantially, as illustrated here across urban (Pretoria), coastal (Cape Town), and rural (Thohoyandou) environments. DN-PMF remains dependent on accurate meteorological characterization, and normalization may introduce bias if applied uniformly across chemically or physically diverse sources. Accordingly, DN-PMF should be implemented as an extension of, rather than a substitute for, standard PMF to support transparency, reproducibility, and comparability across receptor-modelling studies in heterogeneous atmospheric settings. Figure 1 provides the geographical context of the study sites, which differ in meteorological characteristics, seasonal patterns, and socio-economic drivers (Adeyemi et al. 2021; Novela et al. 2020; Williams, Petrik, and Wichmann 2021).

### 1.1. What is New in This Re-Analysis?

This study does not present new $PM_{2.5}$ measurements, but instead applies DN-PMF as a structured sensitivity analysis to three previously published datasets from Pretoria (urban–industrial), Cape Town/Kraaifontein (coastal), and Thohoyandou (rural). By re-analysing these datasets using a consistent dispersion-normalization framework, the study examines how accounting for meteorological dilution influences source interpretation across contrasting environments. Compared with the original PMF-only analyses, this re-analysis provides new insight into the robustness and comparability of PMF source attribution in multi-site studies affected by heterogeneous dispersion regimes, without claiming improved accuracy or source validation.

**Table 1.** Previous studies using receptor source apportionment.

| Authors (year, location) | PM type & Avg. concentration | Species tracked | Model | Key source contributions |
|---|---|---|---|---|
| Chen et al. (2022) New York City, USA | $PM_{2.5}$: 11.1 $\mu g/m^3$ (Bronx) 10.8 $\mu g/m^3$ (Manhattan) 8.7 $\mu g/m^3$ (Queens) | 24-h $PM_{2.5}$ + EC, OC, ions, trace elements | DN-PMF *vs.* PMF | SS (22–28%), SN (10–13%), Gasoline (17–19%), Diesel (up to 12%), Biomass (3–4%), RO (4–6%), Sea salt |
| Cheong et al. (2024) Seoul, Incheon, Gwangju | $PM_{2.5}$: Seoul: 24.2 $\mu g/m^3$ Incheon: 24.6 $\mu g/m^3$ Gwangju: 18.9 $\mu g/m^3$ | $PM_{2.5}$, OC, EC, ions, 20 trace elements | DN-PMF | Secondary nitrate dominant (~40–46%), sulfate (12–15%), biomass burning, mobile, incinerator |
| Ryoo et al. (2025) Beijing & Baoding, China | $PM_{2.5}$: Beijing: 46.6 $\mu g/m^3$ Baoding: 76.5 | OC, EC, ions, trace elements | DN-PMF | Beijing: Secondary nitrate (37.3%), sulfate (16.4%), mobile (15.7%) Baoding: Biomass/residential heating (27.1%), nitrate (22.5%) |
| Jeong et al. (2022) Seoul & Beijing | $PM_{2.5}$ (no avg. given) | OC, EC, trace metals, ions | DN-PMF & PMF | Seoul: Nitrate (25.5%), sulfate (20.5%) Beijing: Nitrate (31.7%), sulfate (17.6%) |
| Kim et al. (2024) South Korea (3 cities) | $PM_{2.5}$ (daily data, no avg. given) | Carbon species, trace elements, ions | DN-PMF | Improved spatial–temporal apportionment; policy-focused |
| Dai et al. (2024) NY/NJ, USA | $PM_{2.5}$ (10 years, multi-site) | OC/EC, ions, trace elements (speciation network) | DN-PMF | Seasonal variation captured; urban *vs.* rural source contrast |
| Howlett-Downing et al. (2024) Pretoria, South Africa | $PM_{2.5}$ = 23.2 ± 17.3 $\mu g/m^3$ | $PM_{2.5}$ trace elements | PMF + HYSPLIT | Mining (33%), dust (24%), industry (15%), vehicular (12%), and biomass (4%) |
| ACP et al. (2024) Montréal, Canada | $PM_{2.5}$ (80 samples) | OC, EC, ions, metals (Fe, Pb, Cd), levoglucosan | PMF | Health risk focus; biomass, vehicle, industrial, and secondary sources |

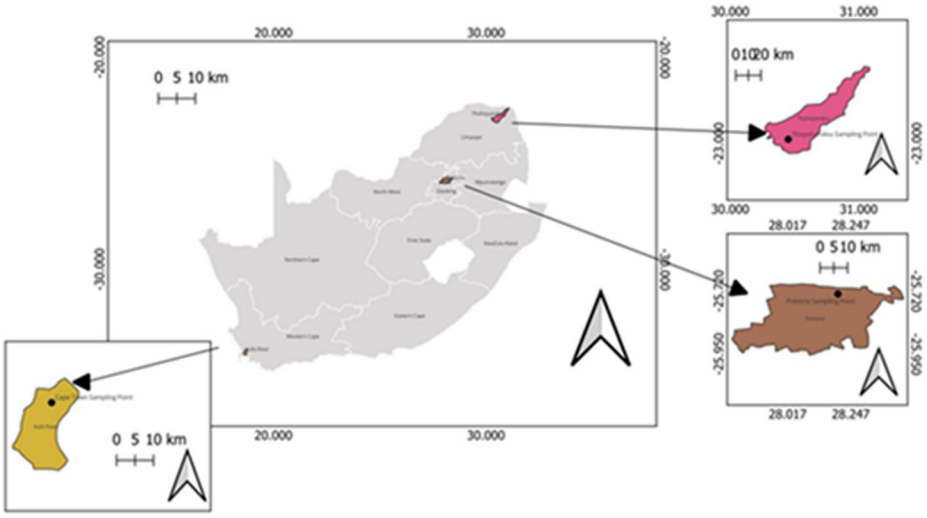


**Figure 1.** The three sampling sites for ambient total $PM_{2.5}$, Cape Town (−18.70S and 33.84E), Thohoyandou (−23.00S and 30.11E), and Pretoria (−25.73S and 28.19E), 2017–2018.

The first object of the project is to establish a trend in the sampled $PM_{2.5}$ and constituent trace elements. The second objective of the project is to determine the number of the main sources of total $PM_{2.5}$ by means of PCA (SPSS). The third objective is to refine the assignment of sources to factors by means of the conventional PMF (EPA PMF 5.0). The DN-PMF will run to confirm the allocation of sources to factors and serve as a sensitivity analysis. Ethics reference No: 68/2022.

## 2. Methods

This study uses previously collected and published $PM_{2.5}$ datasets from three South African cities (Pretoria, Cape Town, and Thohoyandou, 2017–2018). The focus is not on new sampling but on re-analysis using DN-PMF as a sensitivity test to conventional PMF. The analytical and sampling protocols have been described in detail in the studies, and are summarized here for completeness.

### 2.1. Secondary Data Preparation

Briefly, the sampling of ambient $PM_{2.5}$ by gravitation method followed the EPA MLD 055 as used in the ULTRA studies. Ambient $PM_{2.5}$ filter samples were collected manually every third day from 16 April 2017 to 16 April 2018. Samples were collected on 37 mm PTFE membrane filters (Zefon International, Ocala, FL) using GilAir-5 personal air samplers (Sensidyne, Schauenburg Electronic Technologies Group, Mulheim-Ruhr, Germany). The flow rate was 4 L $min^{-1}$. Sampling started 9 am and ended 9 am the next day. The sampling method follows previous studies utilizing gravimetric sampling methods.

An XEPOS 5 energy-dispersive X-ray fluorescence (EDXRF) spectrometer (Spectro analytical instruments GmbH, Kleve, Germany). The EDXRF spectra were processed and quantified using the Spectro XRF Analyzer Pro software. All $PM_{2.5}$ filter samples were analyzed using a total time of 3000 s, automatically divided between the four analytical setup conditions. The concentrations of the following 21 elements were analyzed for: As, Ba, Br, Ca, Cl, Cu, Fe, K, Mn, Ni, P, Pb, S, Sb, Se, Si, Sr, Ti, U, V, and Zn.

### 2.2. Precision Was Estimated Using the Root Mean Square Method on the Duplicate Sample Concentration

The data preparation stage closely follows the recommendations of Reff, Eberly, and Bhave (2007) (Reff, Eberly, and Bhave 2007). Twenty-three trace elements were sampled by means of XRF as discussed in methods chapter. Ten trace elements as well as Cu and U were included in the PMF model. These include Br, Ca, Cl, Cu, Fe, K, Ni, S, Si, Ti, U, and Zn. Every 5th sample was a duplicate and the precision was calculated by using the root mean square method. The factors were tested for independence and seasonality by means of a Kruskal–Wallis test (H0: $\mu1 \neq \mu2 \neq \mu3 \neq \mu4$) using STATA version 18 (College Station, TX). A Spearman's Rank Correlation test was performed to test correlations between factors. This is a test for independence.

### 2.3. Conventional Positive Matrix Factorization

The initial receptor source apportionment was conducted using the C-PMF receptor model, version 5.0,

developed by the U.S. Environmental Protection Agency (EPA). C-PMF is a multivariate factor analysis technique that estimates both source profiles and their contributions using a weighted least squares approach.

In C-PMF, the observed data matrix **X** (with dimensions $n$ samples by $m$ species) is mathematically decomposed into two unknown matrices:

**G** ($n \times p$), representing source contributions for each sample

**F** ($p \times m$), representing source profiles (chemical composition of each source)

**E**, the residual matrix representing model errors

The model solves the equation:

$$X = GF + E \quad (1)$$

The number of factors, $p$, is unknown and must be estimated. The solution is obtained iteratively by minimizing the objective function (Q-value), which quantifies the model fit: where: ($e_{ij}$) = residuals (observed − modelled concentrations), ($s_{ij}$) = measurement uncertainties, and Q = fit quality parameter

$$Q(E) = \sum_{i=1}^{m}\sum_{j=1}^{n}\left(\frac{e_{ij}}{s_{ij}}\right)^2 \quad (2)$$

### 2.4. Selection of Number of Factors and Source Identification

Deciding on the number of factors and assigning the sources to the determined factors introduces both model and conceptual uncertainty. Within the C-PMF run, this is typically done by assessing multiple statistical indicators, such as the Q-value trends, residual distributions, and Signal-to-noise (S/N) ratios. Principal Component Analysis (PCA) using IBM SPSS will support the choice of the overall number of factors using the k-means test. A Spearman's Rank Correlation test can confirm separation of factors and thus sources.

Subjective bias can be introduced when assigning the sources to factors. This choice strongly depends on the correlations between elements within the matrix (initial test) and previous literature. The final source-factor configuration is compared with known local source profiles to assign real-world meaning to each factor (Howlett-Downing et al. 2022).

### 2.5. Signal-to-Noise Ratio Classification

To assess the reliability of each species in the model, the S/N ratio ((S) = meaningful signal, and ($N$) = background noise) is calculated:

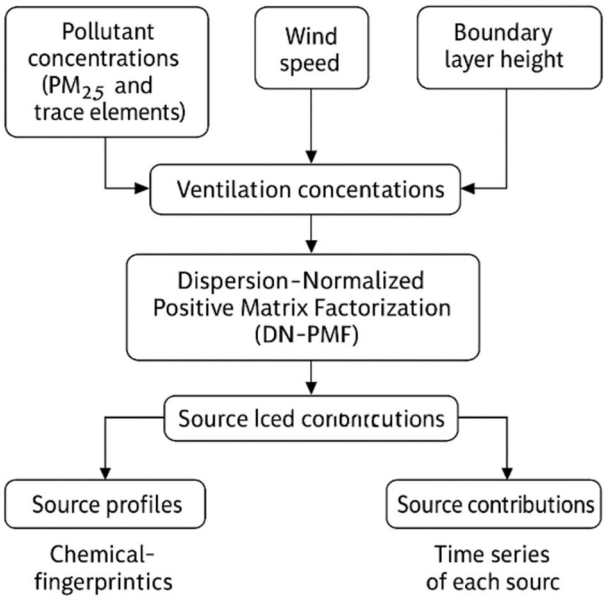


**Figure 2.** The schematic outline of the C-PMF to DN-PMF modelling process.

$$\left(\frac{S}{N}\right)_j = \frac{1}{n}\sum_{i=1}^{n} d \quad (3)$$

Based on the S/N value, species are categorized as: Strong: $S/N > 2$, Weak: $1 < S/N \leq 2$, and Bad: $0.5 < S/N \leq 1$. Species with $S/N < 0.5$ are excluded. Weak species are retained but their uncertainties are tripled. Time series plots of observed *vs.* predicted values are also used to validate the species' classification (Hopke et al. 2020).

### 2.6. Data Pre-Treatment and Uncertainty Estimates

Before modelling: Elemental mass concentrations are converted to their mean oxidized forms. Values below the detection limit (DL) are replaced with half the DL. Associated uncertainties are assigned as 5/6 of the DL.

### 2.7. Model Setup and Factor Interpretation

C-PMF was run with five to seven factors. The bootstrapping, displacement, and bootstrap-displacement (BS-DISP) techniques were used to evaluate the robustness and stability of the factor solutions.

### 2.8. Dispersion Normalization – Positive Matrix Factorization

DN-PMF has been recently used to reduce the meteorological influences by using the period-specific

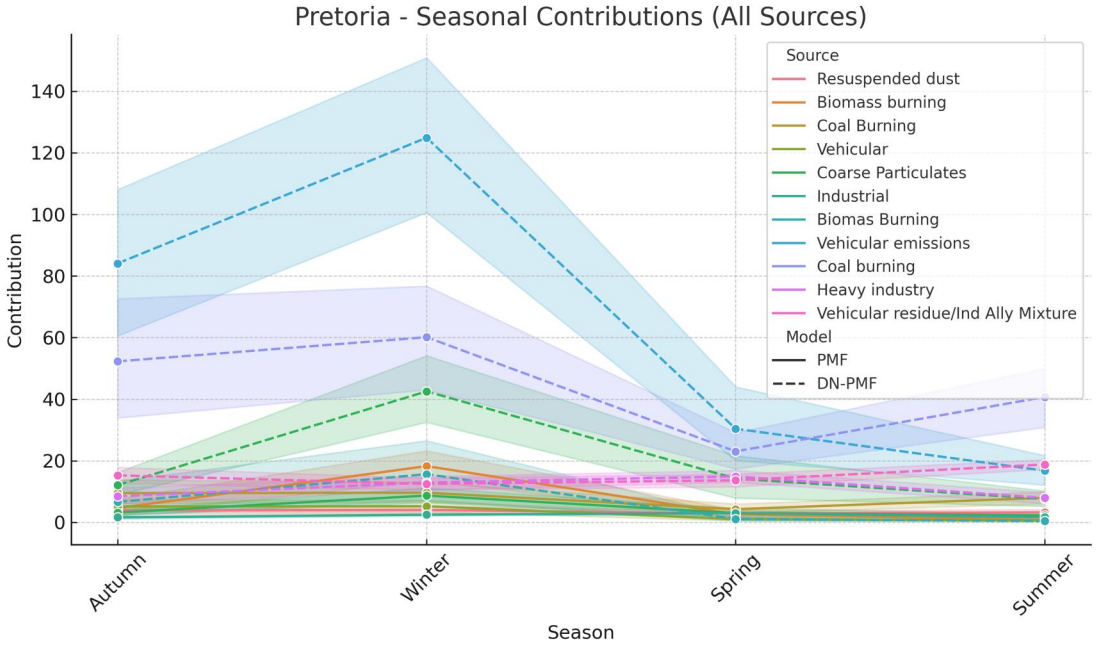


**Figure 3.** The factors (sources) as produced by the C-PMF and the DN-PMF after being conditioned for the VC at the Pretoria site, 2017–2018.

ventilation coefficients (VCs). As described in Dai et al. (2020), VC values were calculated by multiplying MLH for period i with the wind speed ($m.s^{-1}$) for period i ($u_i$).

$$Vc_i = MLH_i \text{ x } u_i \quad (4)$$

Then, dispersion normalized concentrations ($CVC_{,i}$) can be calculated to reduce the influence of local dispersion on the concentrations. $CVC_{,i}$ values are calculated by multiplying the measured concentration ($C_i$) during period i by $VC_i/VC_{mean}$, where $VC_{mean}$ is the mean of period-specific VC values over the whole study period (Figure 2).

$$CVC_i = C_i \text{ x } VC_i/VC_{mean} \quad (5)$$

LIDAR data was used to provide measured MLH values for the three sites. Modelled MLH values were downloaded from Copernicus website (https://cds.climate.copernicus.eu/) and used for the South African sites (Dai et al. 2020).

### 2.9. $PM_{2.5}$ Sampling Sites

Three sites in South Africa representing different meteorological and anthropological activities are being evaluated and compared for their respective health risks for respiratory disorders. Cape Town (−18.70S and 33.84E), Thohoyandou (−23.00S and 30.11E), and Pretoria (−25.73S and 28.19E). These sampling sites are part of a larger program run by the School of Health Systems and Public Health at the University of Pretoria from April 2017 to April 2018. These were the first year-long sampling campaigns conducted by PhD students. The program is ongoing (Molnár et al. 2017) (Figure 3).

The factors (sources) as produced by the C-PMF and the DN-PMF after being conditioned for the VC at the Pretoria site, 2017–2018.

### 2.10. $PM_{2.5}$ Sampling by Gravimetric Methods and Chemical Analysis of Filters by XRF

The sampling regime included 24-h samples collected every third day from 9:00 to 9:00 am the next day using GilAir-5 personal air samplers with 2.0 µm PFTE (Zefluor) 37 mm filters (Zefon International, Inc., Ocala, FL 34474), between 18 April 2017 and 28 February 2020. The total dataset included 123 $PM_{2.5}$ filter samples with 15 duplicate samples.

Gravimetric analyses of $PM_{2.5}$ filters were carried out using a 1 µg sensitivity microbalance (Mettler Toledo, XP6) under climate-controlled conditions (temperature and relative humidity were maintained at 21 ± 0.5 °C and 50 ± 5%, respectively) at the Air Quality Laboratory, SHSPH. The elemental composition of aerosol particles on all filters was determined using an XEPOS 5 EDXRF spectrometer (Spectro Analytical Instruments GmbH, Kleve, Germany) at the Department of Chemistry and Molecular Biology, Atmospheric Science Division, University of Gothenburg. BC and UV-PM was measured using a Model OT21 Optical Transmissometer (Magee Scientific Corp., Berkeley, CA) (Boman et al.

**Table 2.** Results of the factors from the C-PMF and the DN-PMF models for Pretoria, Cape Town/Kraaifontein and Thohoyandou, 2017–2018.

| Cape Town | Total $PM_{2.5}$ | | | Thohoyandou | Total $PM_{2.5}$ | | | Pretoria | Total $PM_{2.5}$ | | |
|---|---|---|---|---|---|---|---|---|---|---|---|
| Sources | PMF | DN-PMF | % Diff | Sources | PMF | DN-PMF | % Diff | Sources | PMF | DN-PMF | % Diff |
| Secondary S | 0.15 | 0.16 | −0.01 | Biomass burning | 0.134 | 0.178 | −0.044 | Resuspended dust | 0.126 | 0.12 | 0.006 |
| Coarse Particulates | 0.097 | 0.05 | 0.047 | Vehicular emissions | 0.021 | 0.019 | 0.002 | Biomass burning | 0.24 | 0.037 | 0.203 |
| Industry emissions | 0,29 | 0.15 | 0.14 | Vegetative burning | 0.017 | 0.05 | −0.033 | Secondary S | 0.29 | 0.28 | 0.01 |
| Zinc smelter emissions | 0.06 | 0.18 | −0.12 | Coal burning | 0.356 | 0.33 | 0.026 | Vehicular emissions | 0.11 | 0.41 | −0.3 |
| Exhaust emissions | 0.14 | 0.23 | −0.09 | Industrial/mining emissions | 0.26 | 0.264 | −0.004 | Coarse particulate matter | 0.157 | 0,12 | 0.037 |
| Sea Air/Vehicular emissions | 0.093 | 0.12 | −0.027 | Coarse dust | 0.214 | 0.16 | 0.054 | Industrial emissions | 0.078 | 0.066 | 0.012 |
| Biomass Burning | 0.17 | 0.1 | 0.07 | | | | | | | | |

2009; Molnár, Johannesson, and Quass 2014; Molnár et al. 2017).

### 2.11. Statistical Analysis

The descriptive analysis was done with STATA version 18. The factors from the source apportionment analysis were tested for independence and seasonality by means of a Kruskal–Wallis test (H0: $\mu_1 \neq \mu_2 \neq \mu_3 \neq \mu_4$) using STATA version 18. A Spearman's Rank Correlation test was performed to test for correlations between constituents of total $PM_{2.5}$, BC, UV-PM, and trace elements. The factors were also tested for correlations. Factors should not be correlated as this indicated a good separation and thus identification for sources.

## 3. Results

A summary of descriptive statistics of total $PM_{2.5}$, BC, organic carbon (UV-PM), and trace elemental concentrations during the measurement period from 18 April 2017 to 28 February 2020 is given in Supplementary Tables S1–S3. The seasonal descriptive analysis demonstrates how the highest concentrations for total $PM_{2.5}$ are during spring in Cape Town and Thohoyandou and during winter for Pretoria. At all three sites, S is the dominant trace element, Supplementary Tables S4–S15.

### 3.1. Spearman's Rank Correlations Test between the Sampled Total PM2.5, BC, UV-PM, and Trace Elements

The most interesting positively correlated elements in Pretoria where K-CL ($\rho = 0.79$), Cl-Si ($\rho = 0.78$), Zn-Br ($\rho = 0.76$), and Cl-Fe with $\rho = 0.68$ ($p < 0.001$). These are attributed to biomass burning, plastic burning (methylation of a phenol group), and e-waste burning. In Thohoyandou, there was a presence of a strong Br-K ($\rho = 0.81$) which is attributed to biomass and plastic waste burning. The other strong correlations were K-S ($\rho = 0.76$), Fe-K ($\rho = 0.75$), and Ti-K ($\rho = 0.70$) ($p < 0.001$). These are usually attributed to biomass burning and other larger PM. In Cape Town, with less industrial activity and along the coast, above average correlations of Pb-As ($\rho = 0.61$), Fe-Ti ($\rho = 0.64$), and Fe-Ca ($\rho = 0.54$) are present. These present a range of wood burning, iron smelting, and sand particulate sources. At all three sites, a strong Pb-As and Ni-Fe correlation is present which is indicative of iron smelting. Of interest in Thohoyandou is how Ni and Cu have correlation with any other element (Tables S16–S18).

### 3.2. C-PMF and DN-PMF Analysis of the Total Dataset

#### 3.2.1. Pretoria

The C-PMF and DN-PMF models applied to Pretoria revealed marked differences in source attribution and seasonal dynamics. Six sources were identified through PCA and resolved using both C-PMF and DN-PMF. In the C-PMF model, the major contributors included coal burning (mean: 29.0%), biomass burning (24.0%), and resuspended dust (12.6%), with lesser contributions from vehicular emissions (11%), coarse particulates (9.7%), and industrial emissions (8%). These sources followed clear seasonal fluctuations, with coal burning dominant in winter and resuspended dust more pronounced in spring and summer (Table 2).

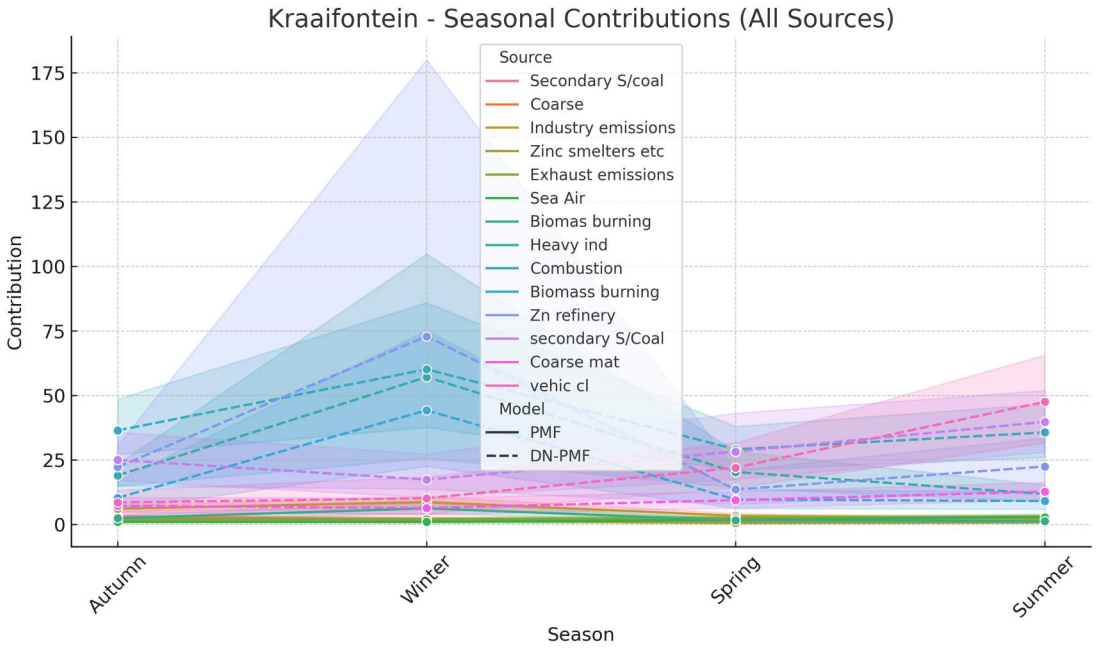


**Figure 4.** The factors (sources) as produced by the C-PMF and the DN-PMF after being conditioned for the VC at the Cape Town/Kraaifontein site, 2017–2018.

In contrast, the DN-PMF model redistributed variance, identifying vehicular emissions (41%), coal burning (28%), coarse particulates (12%), biomass burning (3.7%), and heavy industry (6.6%) as key contributors. The DN-PMF model appeared to suppress biomass burning's contribution compared to the PMF result, while emphasizing vehicular emissions. Tracer diagnostics further indicated a reallocation of Cl and Pb from the C-PMF resuspended dust factor to the DN-PMF biomass source, with a strong Cl-Pb correlation evident.

Spearman rank correlations (not seasonally aggregated) revealed moderate agreement between C-PMF and DN-PMF for coarse particles and coal burning ($\rho = 0.47$–$0.61$, $p < 0.01$), but low correlation for biomass burning, suggesting different factor resolution. DN-PMF captured high winter vehicular source intensity more precisely, likely due to meteorological normalization (Figure 4).

### 3.2.2. Kraaifontein/Cape Town

Seven sources were identified in Kraaifontein. The C-PMF model attributed major contributions to industry emissions (29%), secondary sulphate (15%), biomass burning (17%), and coarse particulates (9.7%). Additional factors included sea salt (9.3%), zinc smelter emissions (6%), and exhaust emissions (14%). PMF seasonality indicated high biomass burning in late winter and spring, with industry emissions peaking in autumn and sea salt highest in summer.

The DN-PMF model similarly resolved seven sources but redistributed contributions. Vehicular emissions (12%), coarse particulates (5%), zinc emissions (18%), biomass burning (10%), and secondary sulphate (16%) were prominent. DN-PMF enhanced vehicular attribution and redistributed sea spray-associated Cl into a mixture with Cu and Zn, indicating vehicular abrasion rather than marine influence (Figure 5).

Correlation analysis showed strong agreement for secondary sulphate ($\rho = 0.82$, $p < 0.001$), moderate agreement for industry emissions ($\rho = 0.53$), and low correlation for sea air and zinc factors, again suggesting meteorological normalization improved vehicular and industrial source resolution.

### 3.2.3. Thohoyandou

Thohoyandou revealed six sources in both models. In the C-PMF model, the dominant contributors were coal burning (35.6%), industrial/mining mixture (26%), resuspended dust (13.4%), and coarse dust (21.4%). Biomass and vehicular emissions were marginal at 1.7% and 2.1%, respectively. The C-PMF seasonal profile indicated coal burning and coarse dust dominance in winter, with industrial emissions stable throughout the year.

DN-PMF restructured the source profile: coal burning remained dominant (33%), but exhaust emissions (17.8%), industry (26.4%), and biomass (5%) gained weight. Resuspended dust (16%) and vehicular emissions (1.9%) remained stable. Interestingly, Cl, previously assigned to vegetative burning in C-PMF was

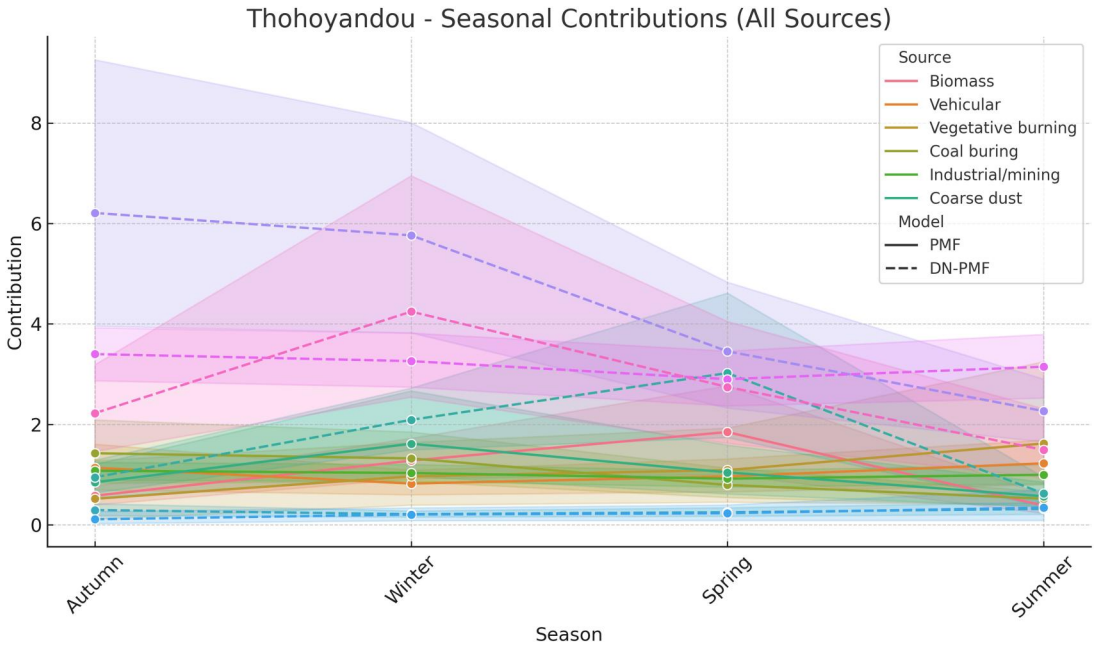


**Figure 5.** The factors (sources) as produced by the C-PMF and the DN-PMF after being conditioned for the VC at the Cape Town/Kraaifontein site, 2017–2018.

reassigned to DN-PMF biomass, showing a stronger Pb-Cl relationship which is more related to methylation of plastics.

## 4. Discussion

### 4.1. Comparison between C-PMF and DN-PMF across Contrasting Atmospheric Environments

In Pretoria, the conventional C-PMF model resolved six distinct sources contributing to $PM_{2.5}$ mass concentrations. The identified sources included coal burning emissions (29%), biomass burning (24%), resuspended dust (12.6%), vehicular emissions (11%), coarse particulates (9.7%), and industrial emissions (8%). The dominant tracers in these profiles were Pb and Cl in the resuspended dust and biomass factors, respectively, with coal burning associated with elevated levels of EC and $SO_4^{2-}$. The resuspended dust factor also carried elements such as Si and Al, characteristic of local soil re-entrainment.

The DN-PMF model identified the same number of sources, but with differences in their contributions and tracer compositions. The DN-PMF model attributed a higher proportion of the $PM_{2.5}$ mass to vehicular emissions (41%), followed by coal burning (28%), coarse particulates (12%), biomass burning (3.7%), heavy industry (6.6%), and mining (9.6%). Unlike the C-PMF model, the biomass factor in DN-PMF featured strong Pb-Cl associations, while Zn and Cu were more prominently linked to the vehicular and industrial sources. This redistribution altered the interpretation of source contributions, suggesting that what was previously identified as resuspended dust in C-PMF may include fine ash and combustion particles under certain dispersion conditions (Table 3).

In Pretoria, this helped distinguish between primary dust events and PM from domestic combustion, particularly during winter months.

The introduction of a separate mining factor in DN-PMF, not clearly resolved with the C-PMF model, may also reflect more nuanced source detection due to the adjustment for intermittent plumes.

At the Cape Town/Kraaifontein site, the C-PMF model resolved seven sources contributing to $PM_{2.5}$, with the following estimated contributions: industry emissions (29%), biomass burning (17%), secondary sulphate (15%), coarse particulates (9.7%), zinc smelter emissions (6%), exhaust emissions (14%), and sea spray (9.3%). Tracer elements for these sources included Cl and Na for sea spray; Zn and Pb for smelter emissions; and K, UV-PMF, and BC for biomass burning. The PMF model associated Cl primarily with sea spray, suggesting a dominant marine influence during certain periods.

The DN-PMF model retained seven source factors but reassigned several tracers and redistributed the contributions. In this model, vehicular emissions emerged as a distinct source (12%), separate from exhaust (23%), while heavy industry contributed 15%, zinc smelting 18%, and coarse particulates 5%.

**Table 3.** Key tracer–tracer correlations, likely sources, and interpretation across study sites.

| Site | Tracer pair | $\rho$ Value | Likely source(s) | DN-PMF interpretation | Supporting literature |
|---|---|---|---|---|---|
| Pretoria | K-Cl | 0.79 | Biomass burning, plastic combustion | Biomass source includes plastic/household combustion | Howlett-Downing et al. (2022) |
| Pretoria | Cl-Si | 0.78 | Waste burning, ash-laden dust | Reassigned from dust to biomass | Dai et al. 2020 |
| Pretoria | Zn-Br | 0.76 | E-waste combustion, mixed metal combustion | Industrial–vehicular source clarified | Dai et al. 2020 |
| Pretoria | Cl-Fe | 0.68 | Mixed waste burning | Cl reallocated to combustion-related factor | Adeyemi et al. (2021) |
| Pretoria | Ni-Fe | — | Iron/metal smelting, metallurgy | Stable industrial source across models | Hopke et al. (2006); Adeyemi et al. (2021); Howlett-Downing et al. (2022) |
| Thohoyandou | Br-K | 0.81 | Biomass burning, plastic co-burning | Improved identification of seasonal biomass combustion | Molner et al. (2014) |
| Thohoyandou | K-S | 0.76 | Domestic fuel burning | DN-PMF separates sulfate from biomass and dust | Pachon et al. (2013) |
| Thohoyandou | Fe-K | 0.75 | Biomass ash mixed with soil | DN-PMF captures composite combustion–dust profile | Pachon et al. (2013) |
| Thohoyandou | Ti-K | 0.70 | Biomass or vegetation ash | DN-PMF improves resolution of seasonal emissions | Pachon et al. (2013) |
| Thohoyandou | Ni-Fe | — | Mining/metallurgy | Consistent industrial source | Molner et al. (2014) |
| Cape Town | Pb-As | 0.61 | Metallurgical emissions | Reassigned from marine to industrial | Alpheus et al. (2022) |
| Cape Town | Fe-Ti | 0.64 | Dust, construction activity | DN-PMF enhances separation of vehicular *vs.* crustal sources | Alpheus et al. (2022) |
| Cape Town | Fe-Ca | 0.54 | Road and soil dust | Assigned to resuspended dust | Williams, Petrik, and Wichmann (2021) |
| Cape Town | Cl-Zn/Cu | — | Marine *vs.* industrial abrasion overlap | Cl reassigned from sea salt to vehicular-industrial source | Alpheus et al. (2022) |

Secondary sulphate remained prominent (16%), and biomass burning was reassigned a lower share (10%). Notably, Cl was no longer associated primarily with sea spray but appeared alongside Zn and Cu in the vehicular and industrial factors.

This shift suggests that the PMF model may have overestimated the marine contribution by aggregating both natural sea salt and vehicular emissions with overlapping tracers during high wind conditions. The DN-PMF model's adjustment appears to have reassigned those periods to traffic-related sources. By considering the output from a DN-PMF model in urban areas, complex mixtures of sea-influenced and anthropogenic emissions can be further queried.

The reduction in biomass burning from 17% in PMF to 10% in DN-PMF is also notable. The output from the DN-PMF's model during the dry months when regional and local fires coincide with increased household fuel use demonstrate the use as a sensitivity test.

The Cl-Zn combination remaining dominant in industrial and vehicular sources under DN-PMF supports a linkage between metallurgy-related emissions and on-road traffic, an association also found in urban receptor modelling by Hopke (2016).

In Thohoyandou, a rural site with limited industrial activity and relatively low traffic volume, both PMF and DN-PMF identified six factors contributing to $PM_{2.5}$. However, differences emerged in how the sources were interpreted and apportioned. The conventional PMF model identified coal burning emissions (35.6%) and an industrial/mining mixture (26%) as the dominant contributors, followed by coarse dust (21.4%), resuspended dust (13.4%), vehicular emissions (2.1%), and vegetative burning (1.7%). Tracers, such as Cl, K, and $SO_4^{2-}$ were prominent in combustion-related factors, while Al and Si were elevated in the dust-related profiles.

In contrast, the DN-PMF model resolved six factors with shifted contributions: coal burning emissions (33%), industry (26.4%), exhaust emissions (17.8%), resuspended dust (16%), biomass burning (5%), and vehicular emissions (1.9%). Notably, coarse dust was not retained as a standalone factor, and a new exhaust-related source was extracted. The DN-PMF

model reassigned Cl to the biomass burning profile, rather than vegetative burning, and redistributed combustion tracers (e.g., EC, $K^+$) across more distinct seasonal source profiles.

While the number of sources remained the same, DN-PMF introduced clearer temporal resolution for exhaust and biomass factors that vary seasonally with household fuel use and agricultural activity.

Importantly, Thohoyandou presented relatively low source complexity, which facilitated cleaner separation of profiles under DN-PMF. Compared to Pretoria or Cape Town, the DN-PMF model performed more distinctly, supporting its value as a sensitivity test in rural settings. This is consistent with the literature, where DN-PMF is often applied in low-to-moderate complexity environments to isolate seasonal or intermittent sources. The emergence of an exhaust-specific factor, not present in PMF, suggests that DN-PMF's dispersion normalization captured episodic traffic contributions, possibly linked to agricultural machinery or seasonal mobility patterns not apparent in PMF's averaged structure.

Taken together, the Thohoyandou results suggest that DN-PMF offers enhanced granularity in environments with relatively simple emissions. Its capacity to resolve seasonal combustion types and better attribute tracer elements reflects its usefulness in rural receptor modelling – particularly where conventional PMF may underrepresent low-intensity but temporally distinct sources.

Pretoria, positioned near South Africa's most polluted regions (Vaal Triangle, Highveld, Waterberg-Bojanala priority areas), represents a complex urban-industrial airshed with overlapping emission sources (Wernecke, Naidoo, and Wright 2023). The presence of vehicular, industrial, mining, domestic fuel, and regional transport signals makes it a particularly challenging case for receptor models. In this setting, DN-PMF did not collapse but revealed reorganization of source contributions: vehicular emissions were elevated, and some tracers (e.g., Pb, Cl) shifted from dust to biomass or traffic-related factors. However, the number of resolved factors remained the same (6), suggesting that while source profiles were reorganized, DN-PMF retained stability.

What this indicates is that DN-PMF did not outperform PMF in resolving new sources, but it did improve interpretability by adjusting for meteorological dilution effects especially under stagnant wintertime conditions. In Pretoria, with dense source overlap, DN-PMF enhanced differentiation between combustion types but did not entirely separate all complex mixtures.

By contrast, Kraaifontein (Cape Town) presents a coastal urban site with seasonal meteorological shifts (winter rainfall and summer sea breeze) and relatively distinct industrial and marine contributions. Here, DN-PMF provided more clearly separated sources. Sea spray was no longer overestimated, and the vehicular and industrial profiles were better differentiated. The method adjusted for wind-driven tracer redistribution, especially Zn, Cl, and Cu, that could otherwise be assigned to multiple sources. The DN-PMF thus captured temporal nuances introduced by seasonal meteorology and complex dispersion regimes typical of coastal settings.

Thohoyandou, a rural site with simpler emission profiles (less traffic, smaller industrial base), provided a cleaner separation between sources in both PMF and DN-PMF. However, DN-PMF still improved factor attribution, e.g., better separating biomass from vegetative burning and highlighting seasonal exhaust emissions that PMF could not resolve. The model did not collapse under sparse conditions and in fact performed best in terms of clarity of source apportionment.

In Pretoria, an urban-industrial node influenced by South Africa's three designated air pollution priority areas, source signatures were highly entangled due to overlapping industrial, vehicular, domestic, and regional emissions. DN-PMF did not increase the number of resolved factors but redistributed key tracer associations (e.g., Pb and Cl) and clarified temporal patterns in vehicular and combustion-related contributions. While full source separation remained constrained, the method enhanced interpretability in a setting characterized by complex mixtures. In Cape Town/Kraaifontein, seasonal meteorology (e.g., winter rainfall and sea breezes) introduced dispersion variability that DN-PMF effectively adjusted for. This resulted in clearer delineation between marine, industrial, and vehicular sources, particularly where shared tracers like Cl and Zn obscured source boundaries in conventional PMF. Thohoyandou, representing a rural context with simpler emissions, yielded the most distinct source profiles under DN-PMF. Here, the model enhanced factor clarity, better separating biomass burning from vegetative sources and capturing seasonal exhaust emissions. Overall, the shifting of dominant tracers under the DN-PMF model demonstrated the complex urban conditions and reported less movement in coastal and rural settings where meteorological normalization enhanced source distinction.

### 4.2. Implications for Receptor-Modelling Methodology

The results across all three sites demonstrate that DN-PMF does not fundamentally alter the number of sources resolved by conventional PMF, nor does it introduce new source categories. Instead, its principal contribution lies in modifying tracer–factor associations and redistributing source contributions under varying dispersion conditions. This indicates that DN-PMF should not be interpreted as a replacement for conventional PMF, but rather as a diagnostic or sensitivity framework that can be used to interrogate the robustness of PMF solutions where meteorological dilution strongly influences concentration variability.

The utility of DN-PMF was found to be context dependent. In complex urban–industrial environments such as Pretoria, DN-PMF improved interpretability by clarifying temporal patterns and redistributing tracers (e.g., Pb and Cl) among combustion and traffic-related sources, but it did not fully resolve all overlapping mixtures. In coastal urban settings such as Kraaifontein, where wind-driven dispersion and marine influences are prominent, DN-PMF was particularly effective in reducing the over-attribution of sea spray and improving separation between industrial and vehicular sources. In contrast, in the rural Thohoyandou setting, where emission complexity is lower, DN-PMF yielded the clearest differentiation between seasonal combustion and exhaust-related sources, highlighting its sensitivity to intermittent and low-intensity emissions.

Taken together, these findings suggest that DN-PMF is most appropriately applied as an extension to conventional PMF in multi-site studies or environments with strong seasonal or spatial variability in atmospheric dispersion. Its value lies in improving interpretability and supporting sensitivity analyses, rather than in increasing source resolution or replacing established receptor-modelling approaches.

### 4.3. Uncertainty and Limitations

The interpretation of DN-PMF results is subject to several sources of uncertainty. First, the dispersion normalization relies on accurate estimates of meteorological parameters, particularly mixing-layer height and wind speed, which may introduce uncertainty when derived from secondary datasets or reanalysis products. Second, the use of dispersion normalization assumes that ventilation metrics adequately capture first-order dilution effects, while other meteorological processes such as long-range transport, precipitation scavenging, or local turbulence are not explicitly accounted for. Third, applying a uniform normalization approach across chemically and physically distinct sources may introduce bias, particularly for secondary aerosols or sources whose formation is not directly proportional to local emissions. For these reasons, DN-PMF should be interpreted as a diagnostic or sensitivity framework rather than a replacement for conventional PMF, and its results should be evaluated alongside traditional source apportionment outputs and site-specific meteorological context.

## 5. Conclusion

DN-PMF's performance as a sensitivity test does not degrade in complex environments since it reorganizes contributions and enhances tracer specificity but its ability to fully separate overlapping sources is constrained when the emission signals are temporally and chemically entangled, as in Pretoria.

Conversely, DN-PMF performs exceptionally well in sites with either distinct source behaviors (Cape Town) or simpler emission profiles (Thohoyandou). This suggests it is a robust method across diverse environments but is most informative where dispersion conditions or source intermittency affect traditional PMF outputs.

## Disclosure Statement

No potential conflict of interest was reported by the author(s).

## ORCID

Chantelle Howlett-Downing http://orcid.org/0000-0002-9398-586X

## References

Adeyemi, A., P. Molnar, J. Boman, and J. Wichmann. 2021. "Source Apportionment of Fine Atmospheric Particles Using Positive Matrix Factorization in Pretoria, South Africa." *Environmental Monitoring and Assessment* 193 (11): 716. https://doi.org/10.1007/s10661-021-09483-3

Alfeus, A., P. Molnar, J. Boman, P. K. Hopke, and J. Wichmann. 2024. "PM2. 5 in Cape Town, South Africa: Chemical Characterization and Source Apportionment Using Dispersion-Normalised Positive Matrix Factorization." *Atmospheric Pollution Research* 15 (3): 102025. https://doi.org/10.1016/j.apr.2023.102025

Boman, J., J. Lindén, S. Thorsson, B. Holmer, and I. Eliasson. 2009. "A Tentative Study of Urban and Suburban Fine

Particles (PM2.5) Collected in Ouagadougou, Burkina Faso." *X-Ray Spectrometry: An International Journal* 38 (4): 354–362. https://doi.org/10.1002/xrs.1173

Chen, Y., D. Q. Rich, and P. K. Hopke. 2022. "Long-Term PM2.5 Source Analyses in New York City from the Perspective of Dispersion Normalized PMF." *Atmospheric Environment* 272: 118949. https://www.sciencedirect.com/science/article/pii/S1352231022000140. https://doi.org/10.1016/j.atmosenv.2022.118949

Dai, Q., B. Liu, X. Bi, J. Wu, D. Liang, Y. Zhang, Y. Feng, et al. 2020. "Dispersion Normalized PMF Provides Insights into the Significant Changes in Source Contributions to PM(2.5) after the COVID-19 Outbreak." *Environmental Science & Technology* 54 (16): 9917–9927. https://doi.org/10.1021/acs.est.0c02776

Hopke, P. K. 2016. "Review of Receptor Modeling Methods for Source Apportionment." *Journal of the Air & Waste Management Association (1995)* 66 (3): 237–259. https://doi.org/10.1080/10962247.2016.1140693

Hopke, P. K., Q. Dai, L. Li, and Y. Feng. 2020. "Global Review of Recent Source Apportionments for Airborne Particulate Matter." *The Science of the Total Environment* 740: 140091. https://doi.org/10.1016/j.scitotenv.2020.140091

Hopke, Philip K., Kazuhiko Ito, Therese Mar, William F. Christensen, Delbert J. Eatough, Ronald C. Henry, Eugene Kim, et al. 2006. "PM Source Apportionment and Health Effects: 1. Intercomparison of Source Apportionment Results." *Journal of Exposure Science & Environmental Epidemiology* 16 (3): 275–286. https://doi.org/10.1038/sj.jea.7500458

Howlett-Downing, C., J. Boman, P. Molnár, J. Shirinde, and J. Wichmann. 2022. "PM2.5 Chemical Composition and Geographical Origin of Air Masses in Pretoria, South Africa." *Water, Air, & Soil Pollution* 233 (7): 1–13. https://doi.org/10.1007/s11270-022-05746-y

Huang, Y., H. Gong, H. Hu, B. Fu, B. Yuan, S. Li, G. Luo, et al. 2021. "Migration and Emission Behavior of Arsenic and Selenium in a Circulating Fluidized Bed Power Plant Burning Arsenic/Selenium-Enriched Coal." *Chemosphere* 263: 127920. https://doi.org/10.1016/j.chemosphere.2020.127920

Hueglin, C., R. Gehrig, U. Baltensperger, M. Gysel, C. Monn, and H. Vonmont. 2005. "Chemical Characterisation of PM2.5, PM10 and Coarse Particles at Urban, near-City and Rural Sites in Switzerland." *Atmospheric Environment* 39 (4): 637–651. https://doi.org/10.1016/j.atmosenv.2004.10.027

Junker, C., and C. Liousse. 2008. "A Global Emission Inventory of Carbonaceous Aerosol from Historic Records of Fossil Fuel and Biofuel Consumption for the Period 1860–1997." *Atmospheric Chemistry and Physics* 8 (5): 1195–1207. https://doi.org/10.5194/acp-8-1195-2008

Kumar, M. K., V. Sreekanth, M. Salmon, C. Tonne, and J. D. Marshall. 2018. "Use of Spatiotemporal Characteristics of Ambient PM2.5 in Rural South India to Infer Local versus Regional Contributions." *Environmental Pollution (Barking, Essex: 1987)* 239: 803–811. https://doi.org/10.1016/j.envpol.2018.04.057

Lee, C. T., S. S. Ram, D. L. Nguyen, C. C. K. Chou, S. Y. Chang, N. H. Lin, S. C. Chang, et al. 2016. "Aerosol Chemical Profile of near-Source Biomass Burning Smoke in Sonla, Vietnam during 7-SEAS Campaigns in 2012 and 2013." *Aerosol and Air Quality Research* 16 (11): 2603–2617. https://doi.org/10.4209/aaqr.2015.07.0465

Liang, X., T. Zou, B. Guo, S. Li, H. Zhang, S. Zhang, H. Huang, et al. 2015. "Assessing Beijing's PM2.5 Pollution: Severity, Weather Impact, APEC and Winter Heating." *Proceedings of the Royal Society A: Mathematical, Physical and Engineering Sciences* 471 (2182): 20150257. https://doi.org/10.1098/rspa.2015.0257

Molnár, P., L. Tang, K. Sjöberg, et al. 2017. "Long-Range Transport Clusters and Positive Matrix Factorisation Source Apportionment for Investigating Transboundary PM2.5 in Gothenburg, Sweden." *Environmental Science: Processes and Impacts*. https://doi.org/10.1039/c7em00122c

Molnár, P., S. Johannesson, and U. Quass. 2014. "Source Apportionment of PM2.5 Using Positive Matrix Factorisation (PMF) and PMF with Factor Selection." *Aerosol and Air Quality Research* 14 (3): 725–733. https://doi.org/10.4209/aaqr.2013.11.0335

Novela, R. J., W. M. Gitari, H. Chikoore, P. Molnar, R. Mudzielwana, and J. Wichmann. 2020. "Chemical Characterisation of Fine Particulate Matter, Source Apportionment and Long-Range Transport Clusters in Thohoyandou, South Africa." *Clean Air Journal* 30 (2): 1–12. https://doi.org/10.17159/caj/2020/30/2.8735

Pachon, J. E., R. J. Weber, X. Zhang, J. A. Mulholland, and A. G. Russell. 2013. "Revising the Use of Potassium (K) in the Source Apportionment of PM2.5." *Atmospheric Pollution Research* 4 (1): 14–21. https://doi.org/10.5094/APR.2013.002

Reff, A., S. I. Eberly, and P. V. Bhave. 2007. "Receptor Modeling of Ambient Particulate Matter Data Using Positive Matrix Factorization: Review of Existing Methods." *Journal of the Air & Waste Management Association (1995)* 57 (2): 146–154. https://doi.org/10.1080/10473289.2007.10465319

Ruuskanen, J., T. Tuch, H. Ten Brink, A. Peters, A. Khlystov, A. Mirme, G. P. A. Kos, et al. 2001. "Concentrations of Ultrafine, Fine and PM2.5 Particles in Three European Cities." *Atmospheric Environment* 35 (21): 3729–3738. https://doi.org/10.1016/S1352-2310(00)00373-3

Wernecke, B., N. P. Naidoo, and C. Y. Wright. 2023. "Establishing a Baseline of Published Air Pollution and Health Research Studies in the Waterberg-Bojanala Priority Area." *Clean Air Journal* 33 (1): 1–12. https://doi.org/10.17159/caj/2023/33/1.14887

Williams, J., L. Petrik, and J. Wichmann. 2021. "PM2.5 Chemical Composition and Geographical Origin of Air Masses in Cape Town, South Africa." *Air Quality, Atmosphere, & Health* 14 (3): 431–442. https://doi.org/10.1007/s11869-020-00947-y